Diameter-Tunable CdSe Nanotubes from Facile Solution-Based Selenization of $Cd(OH)_2$ Nanowire Bundles for Photoelectrochemical Cells

Hee-Sang Shim,[†,‡] Vaishali R. Shinde,[†,‡] Jeong Won Kim,[‡] Tanaji P. Gujar,[§] Oh-Shim Joo,[§] Hae Jin Kim,[||] and Won Bae Kim*[,‡]

Department of Materials Science and Engineering and Program for Integrated Molecular Systems (PIMS), Gwangju Institute of Science and Technology (GIST), Gwangju 500-712, Republic of Korea, Eco-Nano Research Center, Korea Institute of Science and Technology, P.O. Box 131, Cheongryang, Seoul 130-650, Republic of Korea, and Korea Basic Science Institute, Daejeon 350-333, Republic of Korea

Received December 22, 2008. Revised Manuscript Received March 19, 2009

Diameter-tunable CdSe nanotubes are synthesized via a sacrificial template approach in solution phase by reacting $Cd(OH)_2$ nanowire bundles with NaHSe. The sacrificial templates of diameter-controlled $Cd(OH)_2$ nanowire bundles undergo an interdiffusion process between Se^{2-} and Cd^{2+} species, and subsequently core/shell structures of $Cd(OH)_2$/CdSe are formed at intermediate states. The crystalline CdSe hollow nanotubes are finally formed when all Cd reagent sources are chalcogenized with Se in the solution phase, and their diameter can be readily controlled from ca. 20 to 60 nm depending on the dimension of nanowire bundle templates. With heat treatment at 300 °C, crystallinity of the CdSe nanotubes can be enhanced with removal of amorphous selenium present on the nanotube surface, which shows a photo-conversion efficiency of 0.57% in CdSe/polysulfide liquid-junction solar cell along with a bandgap energy of 1.89 eV. A possible scheme for the CdSe nanotube synthesis from the template of $Cd(OH)_2$ nanowire bundles is also proposed in this article.

Introduction

CdSe is one of the most important II−VI semiconductor materials, which has shown interesting optical, electrical, and optoelectronic properties via quantum confinement in nanocrystals,[1,2] thereby being a promising candidate for the potential applications in various fields such as optoelectronics, biosensors, luminescence as a laser diode, solar cells, biomedical labeling, and so forth.[3] Therefore, it is reasonable to expect that the property of CdSe with unique nanostructures would introduce new applications or could enhance the performance of above-mentioned devices. Most of the research with CdSe has been concentrated on quantum nanoparticles, which were synthesized by chemical routes of a bottom-up method,[1,4,5] but recently nanorods,[6] tetrapods,[7] nanoneedles,[8] nanowires,[9] hyper-branches,[10] and their hollow structures[11,12] have been extensively exploited. Since hollow nanotubes of inorganic semiconductors exhibit properties quite different from those of their bulk forms with both characteristics of one dimensional (1D) and two dimensional (2D) nanomaterials, which may fabricate charge transport

* Corresponding author. Tel.: +82-62-970-2317. Fax: +82-62-970-2304. E-mail: wbkim@gist.ac.kr.

† The scientific contributions of H.S.S. and V.R.S. were equivalent, and their relative order in authorship is arbitrary.

‡ Gwangju Institute of Science and Technology.

§ Korea Institute of Science and Technology.

|| Korea Basic Science Institute.

(1) Murray, C. B.; Norris, D. J.; Bawendi, M. G. *J. Am. Chem. Soc.* **1993**, *115*, 8706. Peng, J. A.; Peng, X. *J. Am. Chem. Soc.* **2001**, *123*, 183.

(2) Bawendi, M. G.; Wilson, W. L.; Rothberg, L.; Carrol, P. J.; Jedju, T. M.; Steigerwald, M. L.; Brus, L. E. *Phys. Rev. Lett.* **1990**, *65*, 1623. Murray, C. B.; Kagan, C. R.; Bawendi, M. G. *Science* **1995**, *270*, 1335. Kagan, C. R.; Murray, C. B.; Nirmal, M.; Bawendi, M. G. *Phys. Rev. Lett.* **1996**, *76*, 1517. Empedocles, S. A.; Bawendi, M. G. *Science* **1997**, *278*, 2114. (e) Yu, W. W.; Qu, L.; Guo, W.; Peng, X. *Chem. Mater.* **2003**, *15*, 2854. Yu, D.; Wang, C.; Guyot-Sionnest, P. *Science* **2003**, *300*, 1277. Pradhan, N.; Xu, H.; Peng, X. *Nano Lett.* **2006**, *6*, 720. Shan, C. X.; Liu, Z.; Hark, S. K. *Nanotechnology* **2005**, *16*, 3133.

(3) Lam, N. S.; Wong, K. W.; Li, Q.; Zheng, Z.; Lau, W. M. *Nanotechnology* **2007**, *18*, 415607. Wang, Z.; Finkelstein, K.; Ma, C.; Wang, Z. L. *Appl. Phys. Lett.* **2007**, *90*, 113115. (c) Hodes, G.; Howell, I. D. J.; Peter, L. M. *J. Electrochem. Soc.* **1992**, *139*, 3136. Huynh, W.; Peng, X.; Alivisatos, A. P. *Adv. Mater.* **1999**, *11*, 923.

(4) Katari, J. E. B.; Colvin, V. L.; Alivisatos, A. P. *J. Phys. Chem.* **1994**, *98*, 4109. Trindade, T.; O'Brien, P. *Adv. Mater.* **1996**, *8*, 161. Peng, X.; Wickham, J.; Alivisatos, A. P. *J. Am. Chem. Soc.* **1998**, *120*, 5343. Mastai, Y.; Polsky, R.; Koltypin, Y.; Gedanken, A.; Hodes, G. *J. Am. Chem. Soc.* **1999**, *121*, 10047. Green, M.; O'Brien, P. *Chem. Commun.* **1999**, 2235. Peng, J. A.; Peng, X. *J. Am. Chem. Soc.* **2001**, *123*, 1389. Qu, L.; Peng, Z. A.; Peng, X. *Nano Lett.* **2001**, *1*, 333. Mohamed, M. B.; Burda, C.; El-Sayed, M. A. *Nano Lett.* **2001**, *1*, 589. Chan, E. M.; Mathies, R. A.; Alivisatos, A. P. *Nano Lett.* **2003**, *3*, 199. Chen, X.; Samia, A. C. S.; Lou, Y.; Burda, C. *J. Am. Chem. Soc.* **2005**, *127*, 4372. Sapra, S.; Rogach, A. L.; Feldmann, J. *J. Mater. Chem.* **2006**, *16*, 3391. Park, J.; Joo, J.; Kwon, S. G.; Jang, Y.; Hyeon, T. *Angew. Chem., Int. Ed.* **2007**, *46*, 4630. Das, B. C.; Batabyal, S. K.; Pal, A. J. *Adv. Mater.* **2007**, *19*, 4172.

(5) Palchik, O.; Kerner, R.; Gedanken, A.; Weiss, A. M.; Slifkin, M. A.; Palchik, V. *J. Mater. Chem.* **2001**, *11*, 874.

(6) Chen, C. C.; Chao, C. Y.; Lang, Z. H. *Chem. Mater.* **2000**, *12*, 1516. Manna, L.; Scher, E. C.; Alivisatos, A. P. *J. Am. Chem. Soc.* **2000**, *122*, 12700. Peng, Z. A.; Peng, X. *J. Am. Chem. Soc.* **2002**, *124*, 3343. Fritz, K. P.; Perovic, A.; Nair, P. S.; Petrov, S.; Perovic, D. D.; Scholes, G. D. *J. Cryst. Growth* **2006**, *293*, 203. Sapra, S.; Poppe, J.; Eychmller, A. *Small* **2007**, *3*, 1886. Li, L.; Hu, J.; Yang, W.; Alivisatos, A. P. *Nano Lett.* **2007**, *1*, 349.

(7) Pang, Q.; Zhao, L.; Cai, Y.; Nguyen, D. P.; Regnault, N.; Wang, N.; Yang, S.; Ge, W.; Ferreira, R.; Bastard, G.; Wang, J. *Chem. Mater.* **2005**, *17*, 5263. Wang, Z. Y.; Fang, X. S.; Lu, Q. F.; Ye, C. H.; Zhang, L. D. *Appl. Phys. Lett.* **2006**, *88*, 083102.

(8) Shan, C. X.; Liu, Z.; Hark, S. K. *Appl. Phys. Lett.* **2005**, *87*, 163108. Cheng, J. H.; Chao, H. Y.; Chang, Y. H.; Hsu, C. H.; Cheng, C. L.; Chen, T. T.; Chen, Y. F.; Chu, M. W. *Physica E* **2008**, *40*, 2000.

10.1021/cm8034483 CCC: $40.75
Published on Web 04/16/2009

and increase the active surface,[13] CdSe tubular nanostructures should be also of great interest for potential applications. However, most successful synthesis of CdSe nanotubes has been limited to template-based methods using cylindrical micelles assembled from organic compounds,[12] t-Se nanowires,[14] Sn nanowires,[15] or anodized aluminum oxide (AAO).[16]

There are several approaches to form nanotubes such as preferential self-assembling, rolling of existing thin film,[17] use of hard template like AAO, use of core template (nanowires) to deposit shell material with subsequent removal of the template material by selective etching, and transformation of a solid nanowire through interface reactions in solid−gas or solid−liquid reaction, the so called Kirkendall effect.[18−20] The self template or sacrificial template approach is analogous to the transformation involving the Kirkendall diffusion process. In this strategy, nanowires as the source template are partially or completely converted to desired materials without change of the 1D shape. Therefore, the sacrificial template approach offers advantages such as that (1) the template is consumed during replacement reactions for hollow structured products and thus the size of the product can be tuned with respect to the original template, (2) many reactions take place under mild conditions in solution, so it avoids requirement of sophisticated instruments, (3) relatively pure products can be obtained as compared to the hard-template routes which require additional post-processing procedures to remove the templates and to clean the products, and (4) large-scale synthesis can be achieved in the liquid phase under a mild condition. However, only few 1D nanomaterials have been found to be suitable for nanotubes via the sacrificial templates in comparison with their spherical counterparts.[12,19−24] For example, Li et al. synthesized CdS nanotubes by reacting thioacetamide (TAA) with the $Cd(OH)_2$ nanowires produced from hydrothermal method.[21] Very recently, Qi et al. reported PbSe nanotubes from Se nanotube templates through solution chemistry.[22]

Herein, we report a sacrificial template approach at a low temperature for the synthesis of size-controlled ultralong CdSe nanotubes from the bundled $Cd(OH)_2$ nanowires. The $Cd(OH)_2$ nanowire bundles (NBs) can be selectively and easily grown on substrates at low temperatures through a chemical precipitation method based on the principle of ionic and solubility products.[25] In this approach, the dimension of synthesized $Cd(OH)_2$ nanowire bundles (NBs) can be readily controlled on flat surfaces with a relatively large area, and thereby the size-tunable CdSe nanotubes can be synthesized from the $Cd(OH)_2$ NB templates. The crystalline CdSe nanotubes are characterized by various physicochemical and optoelectronic analysis for their photoelectrochemical application.

Experimental Methods

In a typical synthesis of CdSe nanotubes, the first step is to obtain $Cd(OH)_2$ nanowire bundles (NBs) on substrates. For the synthesis of $Cd(OH)_2$ NBs as the templates, an aqueous solution of 0.1 M $Cd(NO_3)_2$ (Aldrich Chemicals) was prepared, and to this solution an aqueous NH_3 solution (Aldrich, 28%) was added under a constant stirring. A white precipitate was initially observed, which was subsequently dissolved back into solution upon further addition of the NH_3 solution. A pre-cleaned glass substrate was immersed and placed vertically in the solution. The solution was maintained at a pH of approximately 12 and a temperature of 60 °C for 12 h, resulting in the direct growth of $Cd(OH)_2$ nanowire bundles on the glass substrate. The substrate with the deposited $Cd(OH)_2$ nanostructures was then removed from the $Cd(NO_3)_2$ aqueous alkaline bath, washed with deionized water, dried under air, and used as the sacrificial templates for the transformation to CdSe nanotubes. To obtain the diameter-controlled CdSe nanotubes, $Cd(OH)_2$ NB templates were prepared with different growth times. These substrates coated with the $Cd(OH)_2$ NB templates were reacted with an aqueous NaHSe (100 mL) solution for 30 min, which was prepared through adding 20 mM $NaBH_4$ to a Se-dissolved aqueous solution (10 mM), followed by heat treatment at 60 °C for 1 h with refluxing. After the color of the films was changed from white to dark brown with localized red precipitates, as-converted films were removed from the reaction bath. Here we could synthesize the $Cd(OH)_2$ NBs on the substrates having 80 cm^2 area and transform them completely to CdSe NTs. Uniform nanotubes of CdSe were obtained after the reddish amorphous selenium that formed on the nanotube surface during the conversion process was removed by thermal treatment at 300 °C for 1 h under an inert Ar atmosphere.

The morphology and size of $Cd(OH)_2$ NBs, as-converted $Cd(OH)_2$/CdSe core/shell intermediate structures, and CdSe nanotubes (NTs) all were deposited on the glass substrate and were characterized by field emission scanning electron microscopy

(9) Tang, K.; Qian, Y.; Zeng, J.; Yang, X. *Adv. Mater.* **2003**, *15*, 448. Yu, H.; Li, J.; Loomis, R. A.; Gibbons, P. C.; Wang, L. W.; Buhro, W. E. *J. Am. Chem. Soc.* **2003**, *125*, 16168. Grebinski, J. W.; Hull, K. L.; Zhang, J.; Kosel, T. H.; Kuno, M. *Chem. Mater.* **2004**, *16*, 5260. Jeong, U.; Xia, Y.; Yin, Y. *Chem. Phys. Lett.* **2005**, *416*, 246. Zhao, L.; Lu, T.; Yosef, M.; Steinhart, M.; Zacharias, M.; Gösele, U.; Schlecht, S. *Chem. Mater.* **2006**, *18*, 6094. Shan, C. X.; Liu, Z.; Hark, S. K. *Appl. Phys. Lett.* **2007**, *90*, 193123. Singh, A.; Li, X.; Protasenko, V.; Galantai, G.; Kuno, M.; Xing, H.; Jena, D. *Nano Lett.* **2007**, *7*, 2999.
(10) Kanaras, A. G.; Sonnichsen, C.; Liu, H.; Alivisatos, A. P. *Nano Lett.* **2005**, *5*, 2164.
(11) Zhu, J.-M.; Chen, H.-Y. *Adv. Mater.* **2003**, *15*, 156. Hu, Y.; Chen, J.; Chen, W.; Ning, J. *Mater. Lett.* **2004**, *58*, 2911. Yochelis, S.; Hodes, G. *Chem. Mater.* **2004**, *16*, 2740. Peng, Q.; Xu, S.; Zhuang, Z.; Wang, X.; Li, Y. *Small* **2005**, *1*, 216. Liu, B.; Ren, T.; Zhang, J.-R.; Chen, H.-Y.; Zhu, J.-J.; Burda, C. *Electrochem. Commun.* **2007**, *9*, 551. Pan, D.; Wang, Q.; Jiang, S.; Ji, X.; An, L. *J. Phys. Chem. C* **2007**, *111*, 5661.
(12) Rao, C. N. R.; Govindarj, A.; Deepak, F. L.; Gunari, N. A.; Nath, M. *Appl. Phys. Lett.* **2001**, *78*, 1853.
(13) Goldberger, J.; Fan, R.; Yang, P. *Acc. Chem. Res.* **2006**, *39*, 239. Mor, G. K.; Varghese, O. K.; Paulose, M.; Shankar, K.; Grimes, C. A. *Sol. Energy Mater. Sol. Cells* **2006**, *90*, 2011.
(14) Jiang, X.; Mayer, B.; Herricks, T.; Xia, Y. *Adv. Mater.* **2003**, *15*, 1740.
(15) Hu, J. Q.; Bando, Y.; Zhan, J. H.; Liao, M. Y.; Golbergm, D.; Yuan, X. L.; Sekiguchi, T. *Appl. Phys. Lett.* **2005**, *87*, 113107.
(16) Lin, T. J.; Chen, C. C.; Cheng, S.; Chen, Y. F. *Optics Express* **2008**, *16*, 671.
(17) Shen, Q.; Jiang, L.; Miao, J.; Hou, W.; Zhu, J.-J. *Chem. Commun.* **2008**, 1683.
(18) Yin, Y.; Rioux, R. M.; Erdonmez, C. K.; Hughes, S.; Somorjai, G. A.; Alivisatos, A. P. *Science* **2004**, *304*, 711.
(19) Fan, H. J.; Gösele, U.; Zacharias, M. *Small* **2007**, *3*, 1660.
(20) Miao, J.-J.; Jiang, L.-P.; Liu, C.; Zhu, J.-M.; Zhu, J.-J. *Inorg. Chem.* **2007**, *46*, 5673. Huang, T.; Qi, L. *Nanotechnology* **2009**, *20*, 025606.
(21) Li, X.; Chu, H.; Li, Y. *J. Solid State Chem.* **2006**, *179*, 96.
(22) Huang, T.; Qi, L. *Nanotechnology* **2009**, *20*, 025606.
(23) Cölfen, H.; Mann, S. *Angew. Chem., Int. Ed.* **2003**, *42*, 2350. Li, Y.; Wang, Z.; Ma, X.; Qian, X.; Yin, J.; Zhu, Z. *J. Solid State Chem.* **2004**, *177*, 4386.
(24) Tu, K. N.; Gösele, U. *Appl. Phys. Lett.* **2005**, *86*, 093111. Yin, Y.; Erdonmez, C. K.; Cabot, A.; Hughes, S.; Alivisatos, A. P. *Adv. Funct. Mater.* **2006**, *16*, 1389.
(25) Niu, H.; Gao, M. *Angew. Chem. Int. Ed.* **2006**, *45*, 6462.

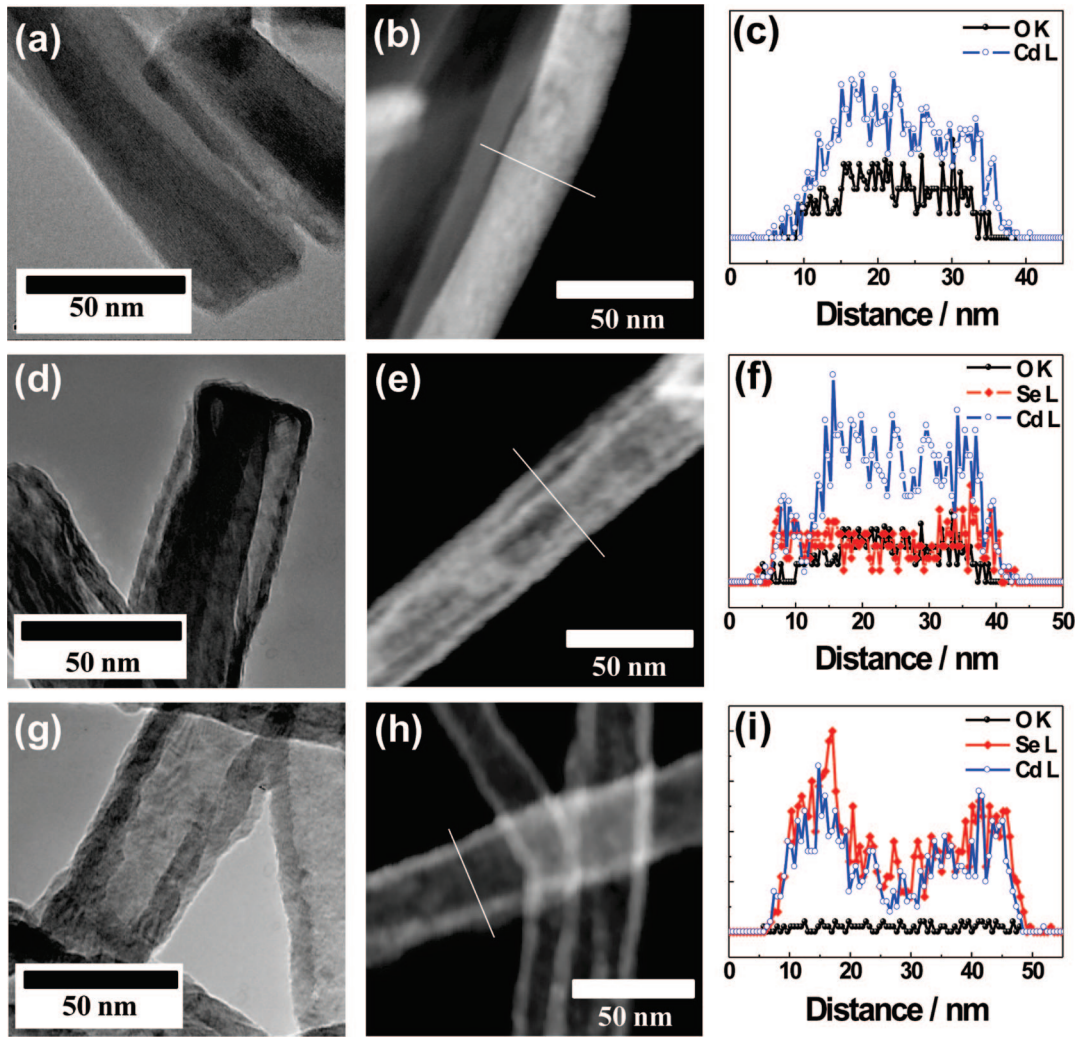

Figure 1. (a, d, g) TEM, (b, e, h) STEM images, and (c, f, i) compositional line profiles: (a−c) $Cd(OH)_2$ NBs, (d−f) intermediate CdSe/$Cd(OH)_2$ core/shell structures, and (g−i) CdSe NTs, respectively.

(FESEM, HITACHI S-4700). For further insight into the microstructure, transmission electron microscopy (TEM), high resolution TEM (HRTEM), and scanning transmission electron microscopy (STEM) observations were performed with a Philips TECNAI F20 TEM unit at an acceleration voltage of 200 kV equipped with Fischione HAADF STEM detector (in KBSI, Korea). The semiquantitative elemental composition of the films was determined from energy dispersive X-ray (EDX) analysis in an energy resolution of 130 eV. The composition and structural identification of the sample deposited on the glass substrate were further investigated by a thermogravimetric analysis (TGA) and a Rigaku X-ray diffractometer using Cu $K\alpha_1$ radiation (λ = 1.5406 Å). Furthermore, the optical and photoelectrochemical properties of CdSe nanotube electrodes were investigated by UV−vis absorption spectroscopy and $J-V$ measurement under dark and in light illumination for photoelectrochemical application. The CdSe photoelectrode cells having an electrode area of 0.49 cm^2 were illuminated using an 1 kW Xenon lamp at a photointensity of 80 mW/cm^2 (AM 1.5G filter). A sputter-deposited thin Pt layer was used as the counter electrode, and 0.2 M polysulfide solution (Na_2S + S + NaOH) was used as the aqueous electrolyte.

Results and Discussion

Figure 1 shows TEM, scanning transmission electron microscopy (STEM) images, and EDX line scanning analyses, which reveal the compositional variation over the $Cd(OH)_2$ NB, intermediate core/shell structure of $Cd(OH)_2$/CdSe, and completely converted CdSe NT, respectively. TEM and STEM images present clear structural changes during the conversion process. $Cd(OH)_2$ NBs used as the sacrificial template in this work show solid wires with a diameter of approximately 35 nm [Figure 1a,b]. Particularly, the bundled nanowires can be clearly seen in the following Figure 2b. The intermediate phase of core/shell structures is also observed by TEM for the samples immersed in the NaHSe aqueous solution during 30 s as shown in Figure 1d,e. Moreover, the samples reacted with the NaHSe aqueous solution for 3 min reveal tubular structure with a diameter of approximately 45 nm after the complete conversion of $Cd(OH)_2$ NBs [Figure 1g,h]. This structural evolution may correspond to their compositional line profiles taken by EDX analyses marked on the STEM images. $Cd(OH)_2$ NB showing the white solid image on Figure 1b exhibits convex-shaped compositional curves for both Cd and O elements [Figure 1c], while the intermediate core/shell structure shows a somewhat complicated concentration profile; both Cd and Se exhibit the relatively higher intensities at the fringes than in the center region, whereas the oxygen component shows

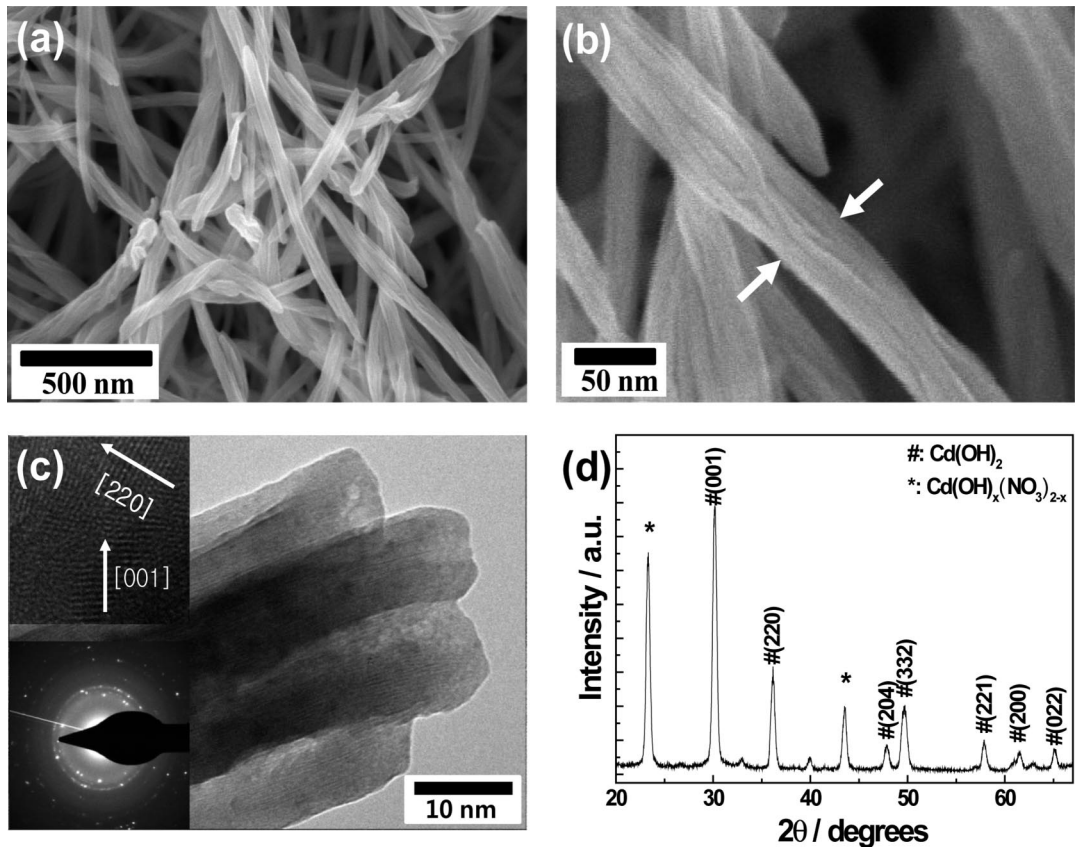

Figure 2. (a, b) Low and high magnification FESEM images, (c) TEM images, and (d) XRD pattern of $Cd(OH)_2$ NBs, respectively. The insets in Figure 2c display the HRTEM image and the SAED pattern of $Cd(OH)_2$ NBs, respectively.

Scheme 1. Schematic Illustration for the Conversion Processes from Bundled $Cd(OH)_2$ Nanowires to CdSe Nanotubes by Reaction with an Aqueous Solution of NaHSe

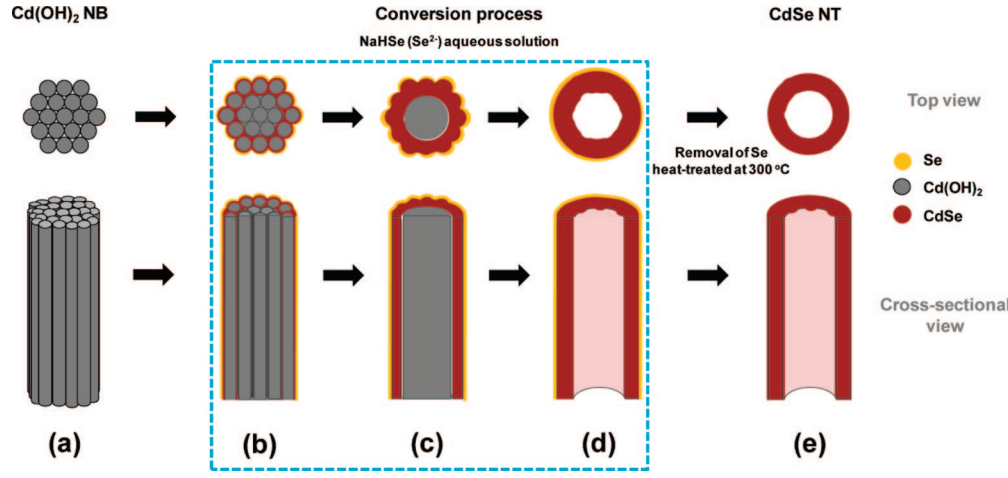

a center-enriched profile [Figure 1f]. When it is immersed into the NaHSe aqueous solution during 3 min for the complete conversion of $Cd(OH)_2$ to CdSe, the $Cd(OH)_2$ core part appears to be absent, and it represents a typical tubular nanostructure of CdSe with a wall thickness of 10−12 nm and an outer diameter of approximately 45 nm as shown in Figure 1h. More interestingly, compositional line profiles of this sample clearly display that the oxygen component disappears and intensities of Cd and Se elements become stronger at both wall sides as shown in Figure 1i.

Scheme 1 illustrates a possible process for the synthesis of CdSe nanotubes from the bundled $Cd(OH)_2$ nanowires used as a new template structure in this work. Scheme 1a represents the template of $Cd(OH)_2$ nanowire bundles (NBs) grown on substrates through a soft solution chemistry as reported in ref 26. When the $Cd(OH)_2$ NBs are reacted with an aqueous NaHSe, interdiffusion of Se^{2-} anions and Cd^{2+} cations occurs through the surface of $Cd(OH)_2$ NBs, and outer shell layers of CdSe begin to form [Scheme 1b]. Then, the decomposed OH^- ions would be dissolved into the

(26) Shinde, V. R.; Shim, H.-S.; Gujar, T. P.; Kim, H. J.; Kim, W. B. *Adv. Mater.* **2008**, *20*, 1008.

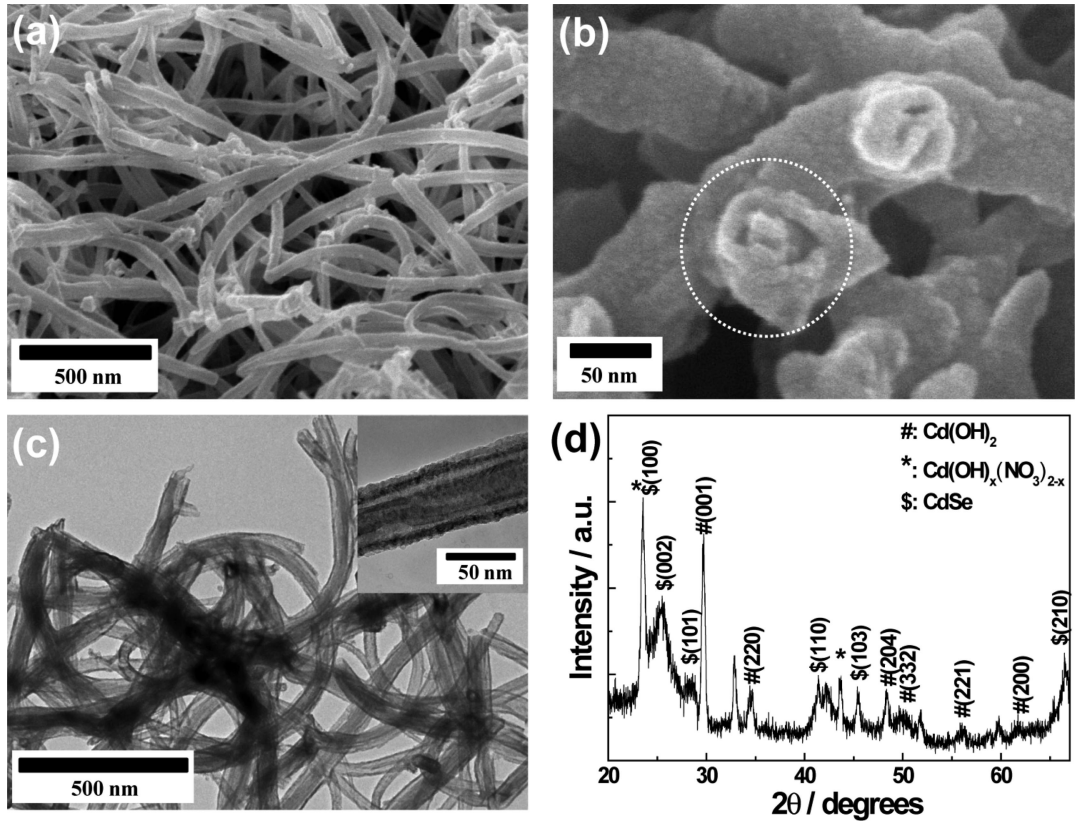

Figure 3. (a, b) Low and high magnification FESEM images, (c) TEM images, and (d) XRD pattern of CdSe/$Cd(OH)_2$ intermediate core/shell structures. Inset figure in part c shows the high-magnified TEM image of the intermediate core/shell structure.

aqueous solution. Intermediate phases having core/shell structures of $Cd(OH)_2$/CdSe are in turn formed as shown in Scheme 1c. It is worthy of noting that the bundled structures with $Cd(OH)_2$ nanowires may provide more efficient inner and outer pathways for diffusion of Se^{2-} ions and Cd^{2+} ions, respectively, than single wire structure cases.[19,23] During this Kirkendall diffusion process, the chemical potential difference of the Cd source between the inside and the outside of the solid phase can provide a driving force for the outward diffusion of the Cd^{2+} ions. Then, Se^{2-} ions supplied from the solution phase form the CdSe shell layer by reacting with Cd^{2+} dominantly on the surface of the template material. When the Cd^{2+} species outdiffused from the $Cd(OH)_2$ core is mostly consumed, an excess amount of Se^{2-} may be possibly deposited onto the surface layers of the formed CdSe NTs [Scheme 1d]. Finally, pure CdSe NTs can be obtained by heat treatment at 300 °C under an inert Ar atmosphere to remove the surface amorphous selenium (a-Se) from the tubular structures [Scheme 1e].

$Cd(OH)_2$ NBs used as the sacrificial templates in this work were prepared by soft solution chemistry under the optimized conditions reported previously.[26] Figure 2 shows microscopy images and the X-ray diffraction (XRD) pattern for the $Cd(OH)_2$ NBs grown on a glass substrate. A low-magnification FESEM image reveals that a large quantity of nanowires was produced on the substrate with lengths ranging up to several tens of micrometers. The nanowires appeared to be randomly distributed on the substrate surface with diameters of 60 ± 10 nm. Interestingly, a high-magnification FESEM image reveals that the individual nanowires are actually constituted (i.e., bundled) of several smaller nanowires having 6−9 nm diameter [Figure 2b], which are about a seventh to tenth of the diameter of the nanowire bundles. TEM image observations on the NB indeed indicate that the smaller nanowires with diameters less than 10 nm are bound together to form the bundle morphology as shown in Figure 2c. The HRTEM image and selective area electron diffraction (SAED) of an individual small wire, as shown in the insets in Figure 2c, indicate that the $Cd(OH)_2$ nanowires produced here have a polycrystalline phase with the SAED pattern containing diffused rings and spots. The interplanar spacings have been measured to be about 2.477 Å and 4.948 Å, which are in a good agreement with the (220) and (001) crystalline planes of monoclinic $Cd(OH)_2$. The phase identification of the sample formed on the glass substrate has been carried out again using XRD measurement, in which the diffraction peaks are unambiguously indexed to the monoclinic phase of $Cd(OH)_2$ [Figure 2d]. The peaks marked with an asterisk (*) are possibly contributed from cadmium hydroxide nitrate (JCPDS No. 40-1491), which might be generated from the interaction of $Cd(OH)_2$ with NO_3^- anions in the solution as discussed in ref 26.

Figure 3a shows the FESEM image taken after a short time reaction of the $Cd(OH)_2$ NBs template with the NaHSe solution for 30 s, in which a morphological change can be inferred as compared to that in Figure 2a. The figure shows that the bundled structure seems to have vanished, and single wire-like or core/shell-like structures are formed, which can be interpreted by the enlarged cross-sectional FESEM image of Figure 3b. Interestingly, the TEM images in Figure 3c for this intermediate structure also support such core/shell-like structures. Some of empty spaces inside might be formed

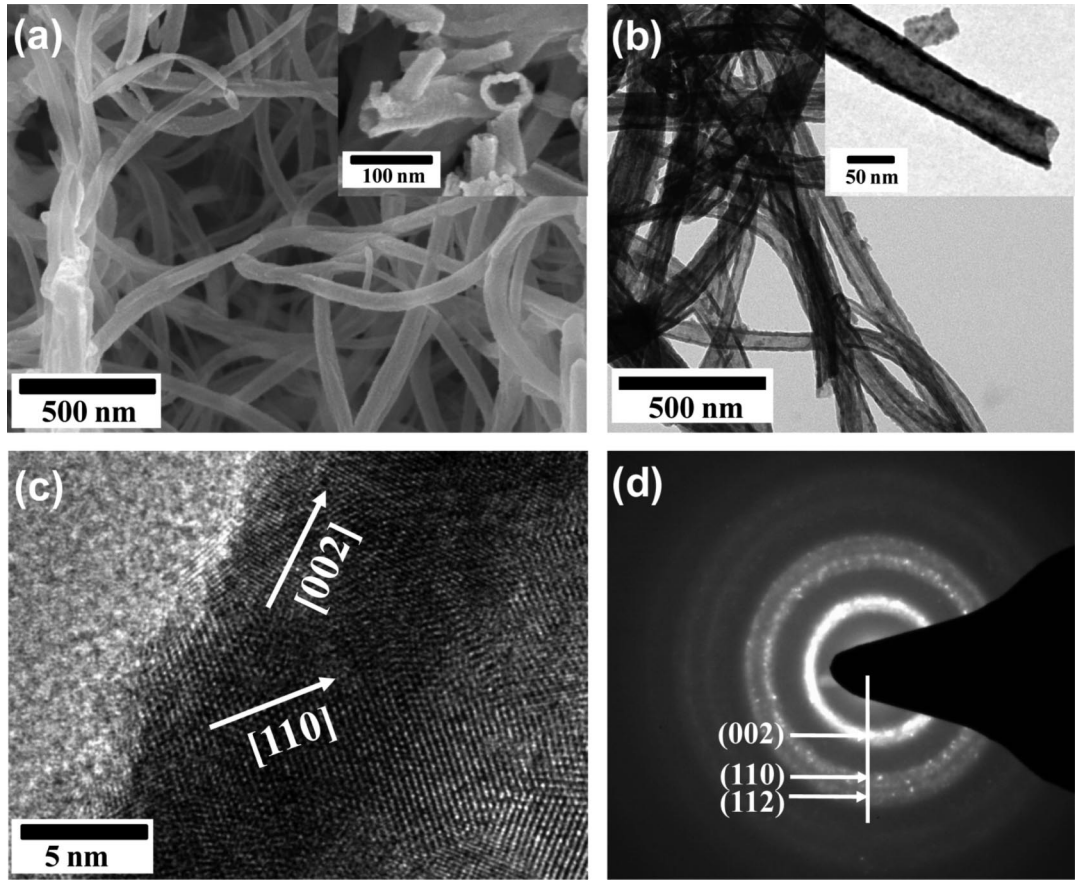

Figure 4. (a) FESEM, (b) TEM, (c) HRTEM, and (d) electron diffraction pattern images of CdSe NTs transformed from $Cd(OH)_2$ nanowire bundles. Inset in part b reveals the high-magnified TEM image of single nanotubes.

due to the different rates of diffusive reactions and/or from the intrinsic inter-spaces present in the nanowire bundle structures. The XRD pattern taken on these intermediate structures after the reaction of 30 s appears to evolve two separate phases of the reactant $Cd(OH)_2$ and the product CdSe. The relatively higher abundance of $Cd(OH)_2$ phase at this stage could indicate that the transformation reaction occurred just on the surfaces of the $Cd(OH)_2$. The formation of the intermediate phases like $Cd(OH)_2$/CdSe core/shell structure can be attributed to an equal or relatively lower outdiffusion rate of the core material than the inward diffusion of the shell phase, since the faster rate of outdiffusion of core material helps to form complete nanotubes. The chemical reaction can be written like reaction 2 below together with the NaHSe formation reaction[27] (reaction 1):

$$2Se + 4NaBH_4 + 7H_2O \rightarrow 2NaHSe + 2Na_2B_4O_7 + 14H_2 \quad (1)$$

$$Cd(OH)_2 + NaHSe \rightarrow CdSe + NaOH + H_2O \quad (2)$$

Figure 4a shows a typical SEM image of the CdSe NTs transformed from $Cd(OH)_2$ NBs in this work, whose samples were treated at 300 °C for 1 h in Ar atmosphere to remove a-Se present on the surface. After the thermal treatment, the 1D nanostructured CdSe with lengths ranging up to several micrometers and diameters having 55 to 70 nm can be seen. Interestingly, the diameter of CdSe nanotubes is slightly but significantly bigger than the template NBs; wall thickness of approximately 10 nm and inner pore diameter of approximately 40 nm can be seen in the insets of Figure 4a,b. TEM image as shown in Figure 4b clearly demonstrates that all $Cd(OH)_2$ NBs were completely converted to the tubular structure of CdSe. The HRTEM image at the walls of CdSe in Figure 4c indicates that the transformed CdSe nanotubes are polycrystalline phase as supported by electron diffraction pattern of Figure 4d.

To further control the diameter of CdSe tubular nanostructures, $Cd(OH)_2$ NB templates were fabricated with respect to different growth times in this work. The diameter and film thickness of $Cd(OH)_2$ NBs formed on glass substrates could be easily tuned by controlling formation time, which is demonstrated in Figure 5a−d, showing the diameter changes from approximately 13 to approximately 41 nm in this work. Figure 5e−h represents FESEM images of their converted CdSe nanotubes. It is obvious that the diameter of CdSe tubular structures strongly depends on the dimension of the original $Cd(OH)_2$ nanowire bundles. All the samples were reacted with the aqueous NaHSe solution for 30 min. The converted sample from $Cd(OH)_2$ NBs with the smallest deposition time of 2 h seems to be different from the others; however, cross-sectional FESEM images indicate clearly that CdSe tubular structures are formed from all the diameter-tuned $Cd(OH)_2$ templates regardless of their

(27) Yamamoto, H.; Oshima, K. *Main Group Metals in Organic Synthesis*; Wiley-VCH, Weinheim, 2006; p 816.

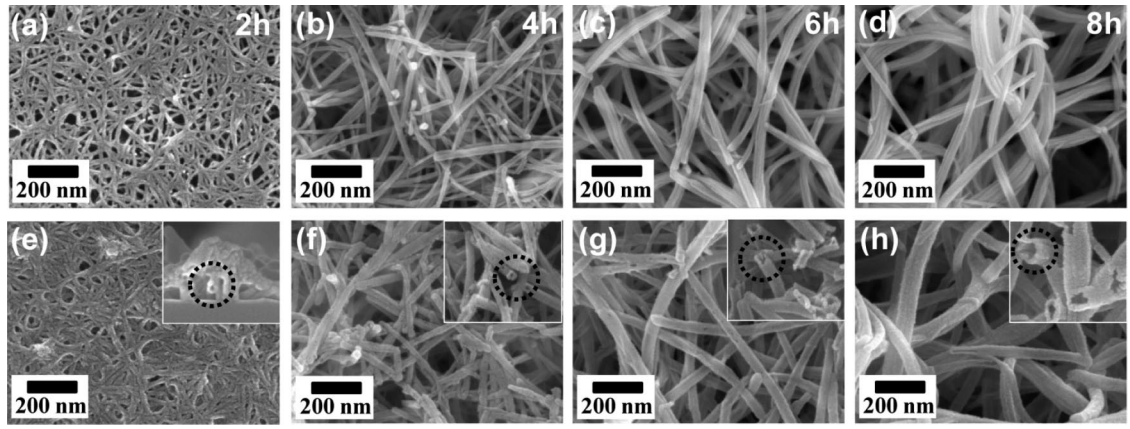

Figure 5. FESEM images of diameter-controlled $Cd(OH)_2$ NBs as the sacrificial templates and their corresponding CdSe NTs fabricated using the $Cd(OH)_2$ NB templates. $Cd(OH)_2$ NBs were obtained with different fabrication times of (a) 2 h, (b) 4 h, (c) 6 h, and (d) 8 h, respectively.

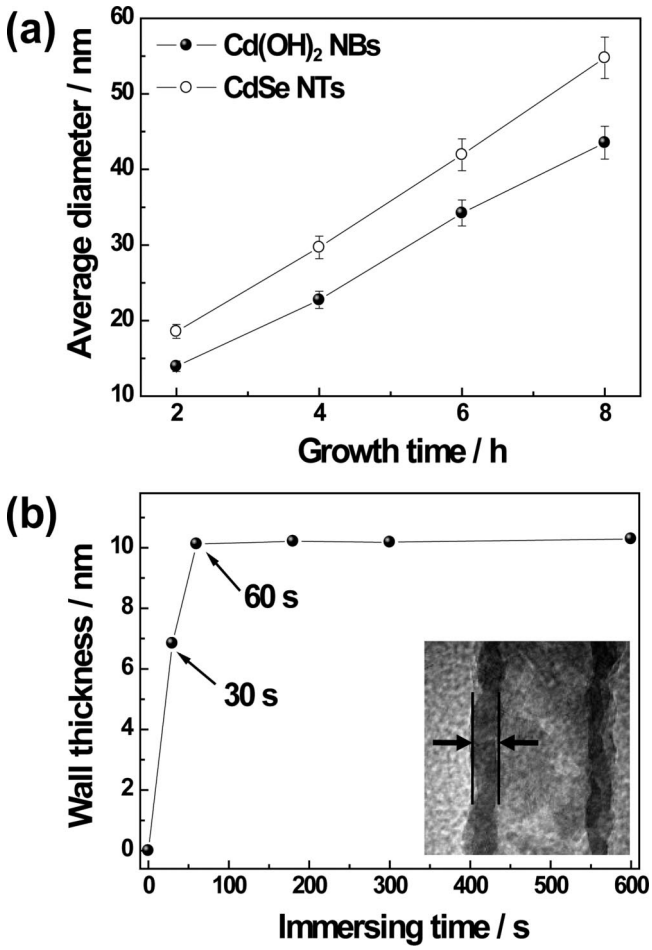

Figure 6. (a) Average diameter change of $Cd(OH)_2$ NBs as a function of the fabrication times and their converted CdSe NTs and (b) wall thickness change of CdSe NTs with different immersing times in the conversion bath.

diameters employed in this work [the insets of Figure 5e−h]. Furthermore, although their wall thickness and surface morphology were slightly varied, hollow 1D structures of CdSe could be also fabricated at temperatures as low as 30 °C via this solution-based conversion process [see the FESEM images in Figure S1, Supporting Information].

Figure 6 summarizes the average diameters of template materials and their converted structures together with the wall thickness of the CdSe. The average diameter and wall thickness of converted structures were estimated using Lince software (Tu Damstadt, Germany) in the error range of 5% here. The average diameters of both the reactant template of $Cd(OH)_2$ NBs and the product of CdSe nanotubes increase proportionally with respect to the growth time from 13 to 41 nm for the template materials and from 18 to 54 nm for the converted materials, respectively [Figure 6a]. The outer diameters of converted nanotubes appear to be slightly smaller than an expected value that is based on non-porous $Cd(OH)_2$ NBs templates, which would be attributed to coalescence of the formed CdSe to minimize the surface energy during the Kirkendall diffusion and the heat treatment process, as mentioned in Scheme 1. For the wall thickness development, we measured the thickness change of CdSe NTs with time over the conversion reaction using the $Cd(OH)_2$ NBs fabricated for 6 h, as shown in Figure 6b. The wall thickness is increased rapidly until 60 s and maintained at the same thickness of approximately 11 nm. It is noteworthy that the outer diameter of converted CdSe NTs is always bigger than the template nanowire bundles, and their diameter difference becomes slightly greater as the diameter of template materials is increased. This result implies that the behavior on such diameter difference is probably understood by the density difference between the nanotube versus nanowire morphology.

It may be possible for an excess of the Se source to be deposited on the CdSe surface in the form of amorphous selenium, particularly after all Cd is reacted with Se. Thermogravimatric analysis (TGA) with XRD results could give the information on the a-Se formation on the CdSe nanotube surface, as shown in Figure 7. The TGA curve was recorded by heating the dry powder of converted CdSe nanotubes in a dinitrogen gas flow from a temperature of 40 to 500 °C at a ramping rate of 5 °C/min. The major weight loss by about 6.4% appears between 200 and 300 °C, which corresponds to the evaporation temperature of selenium that was reported at around 230 °C.[28] Interestingly, the XRD pattern for the sample treated at 300 °C for 1 h under the

(28) Jeong, U.; Xia, Y. *Adv. Mater.* **2005**, *17*, 102. Speight, J. G. *Lange's Handbook of Chemistry*, 16th ed.; McGraw-Hill: New York, 2005. Lide, D. R. *CRC Handbook of Chemistry and Physics*; 86th ed.; CRC Press: Boca Raton, 2006; p 433.

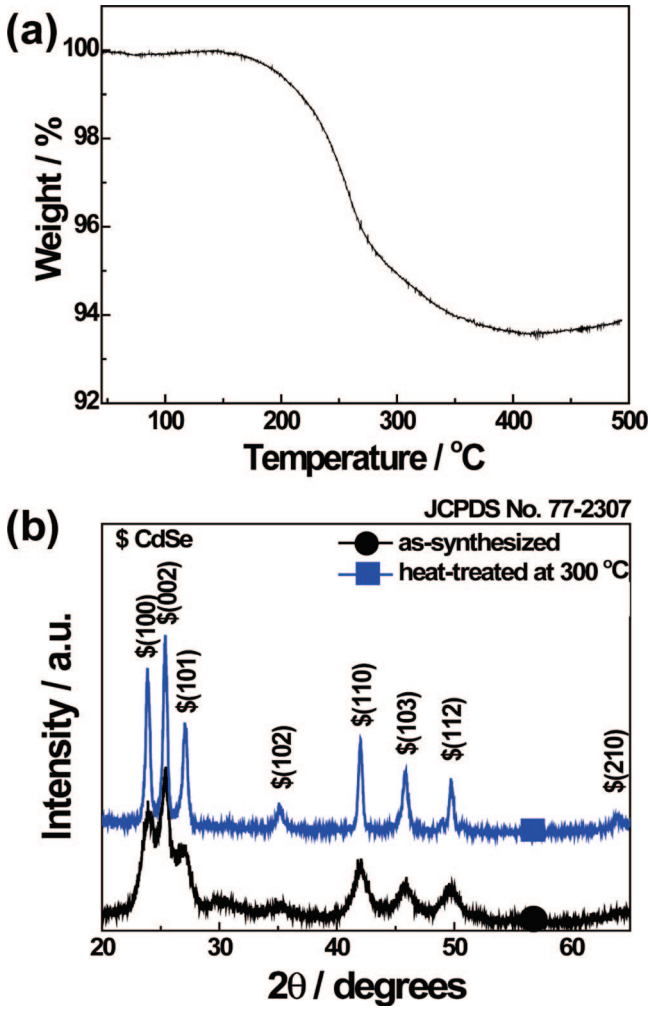

Figure 7. (a) TGA curve of as-synthesized CdSe NTs in a N_2 atmosphere and (b) XRD patterns of as-synthesized and heat-treated CdSe NTs at 300 °C in an Ar atmosphere for 1 h.

inert Ar atmosphere shows stronger crystalline peaks (referred to JCPDS No. 77-2307) as compared to those of as-converted sample [Figure 7b]. These results indicate that the a-Se phase was removed by the thermal treatment along with enhancement of the crystallinity of CdSe NTs. As above-mentioned in the synthetic scheme, the amorphous selenium deposited on the surface of CdSe NTs during the conversion process in this work could be present in a small amount of less than 7 wt %.

Figure 8 shows the UV−vis absorption spectra of $Cd(OH)_2$ NBs template deposited for 4 h and transformed CdSe NTs, which were synthesized on transparent quartz substrates. The absorption of $Cd(OH)_2$ NBs decreases rapidly to the wavelength of 400 nm and then shows a retarded decrease, while CdSe NTs reveal a red-shifted absorption profile from that of $Cd(OH)_2$ NBs showing two peaks at 350 nm and 510 nm, respectively. Optical band gap energy can be determined graphically by rearranging the equation to $(\alpha h\nu)^{1/n} = \text{const}\cdot(h\nu - E_g)$, where n indicates whether the primary optical transition for the light absorption is direct ($n = 0.5$) or indirect ($n = 2$).[29] The linear fitting in the vicinity of the

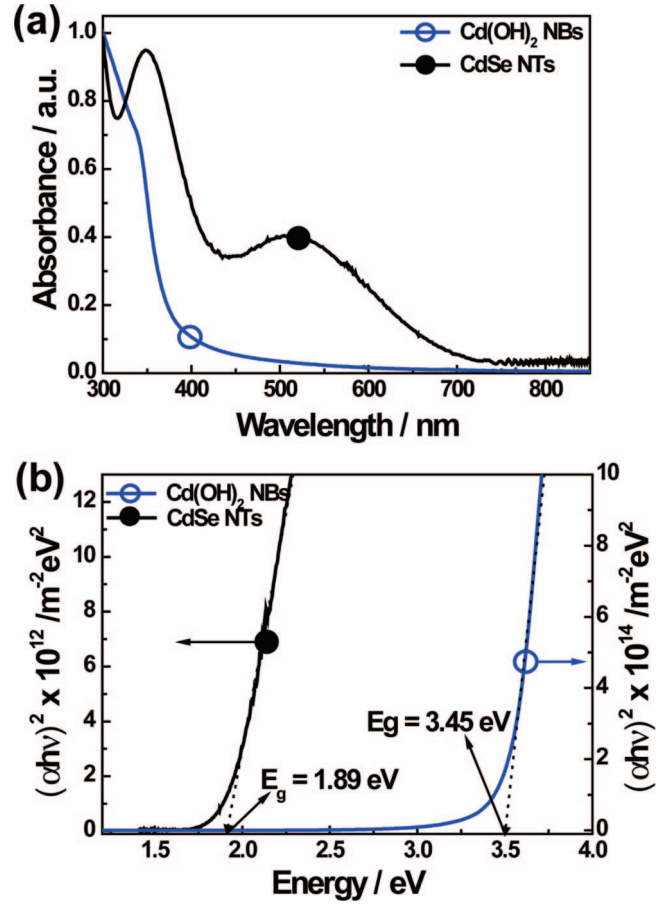

Figure 8. (a) UV−vis absorption spectra and (b) bandgap determination by plotting $(\alpha h\nu)^2$ vs $h\nu$ for $Cd(OH)_2$ NBs and converted CdSe NTs.

bandgap region shows 3.45 eV for the $Cd(OH)_2$ NBs and 1.89 eV for the converted CdSe NTs, respectively, as demonstrated in Figure 8b, which is in a good agreement with other literatures.[30] These results indicate that the CdSe NTs having much smaller band gap than $Cd(OH)_2$ NBs can be used as active photoanode materials to absorb the visible light.

To investigate photoelectrochemical properties of the chemically prepared CdSe NTs via self-templating of $Cd(OH)_2$ NBs in this work, the CdSe nanotube electrodes with the different diameter sizes were compared as a photoanode in photoelectrochemical cells in the form of ITO/CdSe nanotubes/polysulfide electrolyte/Pt under dark and light illumination conditions. The detailed parameters for the photoelectrochemical performance are listed in Table 1. Figure 9 shows the current density versus voltage ($J-V$) curves for the representative cell, which employs the sample converted from 6 h-deposited $Cd(OH)_2$ templates. The open circuit voltage (V_{oc}) with respect to the diameter size of CdSe NTs did not show significant change, but short circuit current density (J_{sc}) and power conversion efficiency (η%) were changed depending on the diameter size up to a 6 h sample from 1.74 to 3.52 mA cm^{-2} and 0.29 to 0.57%, respectively. These results can support that the CdSe NTs have the optimum dimension for the light absorption and the charge

(29) Butler, M. A. *J. Appl. Phys.* **1977**, *48*, 1914.

(30) Kumar, M.; Sharan, M. K.; Sharon, M. *Sol. Energy Mater. Sol. Cells* **1998**, *51*, 35. Shreekanthan, K. N.; Rajendra, B. V.; Kasturi, V. B.; Shivakumar, G. K. *Cryst. Res. Technol.* **2003**, *38*, 30.

Table 1. Performance Parameters of the CdSe Nanotubes with Respect to the Diameter Sizes over Photoelectrochemical Cells

average diameter of CdSe NTs [nm]	V_{oc}qa[V]	J_{sc}[mA cm^{-2}]	fill factor [%]	power conversion efficiency [%]
18.6a	0.337	1.74	45.4	0.29
29.7b	0.311	3.15	43.0	0.53
41.9c	0.312	3.52	40.1	0.57
54.8d	0.308	2.61	36.4	0.37

[a−c] The CdSe nanotubes converted from 2 h, 4 h, 6 h, and 8 h deposited bundled $Cd(OH)_2$ nanowires templates, respectively.

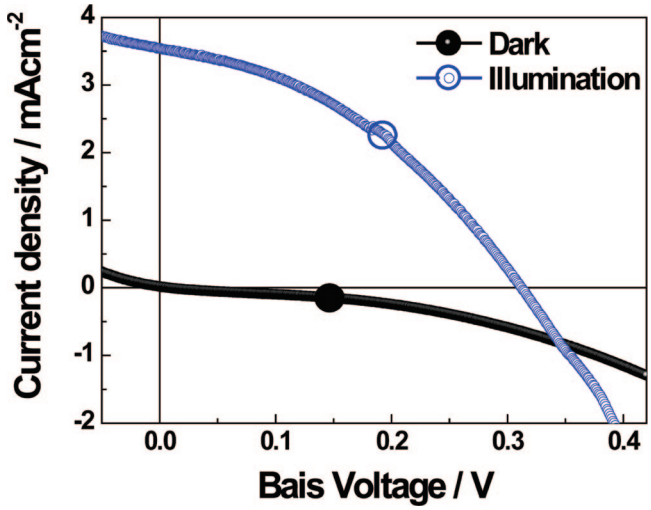

Figure 9. $J-V$ characteristics of CdSe nanotube electrode measured under dark and light illumination at 80 mW cm^{-2} in aqueous polysulfide electrolyte at room temperature.

transport in our tested photoelectrochemical cells. The performance values for the solar cell employing the CdSe NTs in this work are comparable with those of other 1D CdSe nanostructures over the similar photoelectrochemical cells.[31−33] Further optimization and investigation will definitely give a promising application of the CdSe nanotubes from the $Cd(OH)_2$ nanowire bundles as a photoelectrode for the photoconversion devices.

Conclusions

Crystalline CdSe nanotubes have been synthesized via a facile solution conversion process at low temperature by using a sacrificial template of bundled $Cd(OH)_2$ nanowires. This method demonstrated that the diameter-tunable fabrication of CdSe nanotubes can be achieved on a flat substrate. The optical and photoelectrochemical characteristics of the CdSe nanotube electrode fabricated from the $Cd(OH)_2$ nanowire bundles were investigated; the optical bandgap is 1.89 eV, and the photo-conversion efficiency is approximately 0.57 % under 80 mW cm^{-2} illumination. Particularly, the photoelectrochemical performances strongly depend on its diameter size. The method demonstrated here may suggest an efficient fabrication of hollow CdSe nanotubes for use in nanoscale electronic and optoelectonic devices.

Acknowledgment. This work was supported by the Basic Research Program (No. R01-2009-000-10870-0) and NCRC (No. R15-2009-006-03002-0) funded by the Korea Science and Engineering Foundation (KOSEF), and the Hydrogen Energy R&D Center as one of the 21st Century Frontier R&D Program funded by the Korea government (MEST).

Supporting Information Available: Detailed information for preparing NaHSe solution and additional FESEM images of the samples obtained at different processing temperatures (PDF). This material is available free of charge via the Internet at http://pubs.acs.org.

CM8034483

(31) Shaikh, A. V.; Mane, R. S.; Pathan, H. M.; Min, B.-K.; Joo, O.-S.; Han, S.-H. *J. Electroanal. Chem.* **2008**, *615*, 175.

(32) Schierhorn, M.; Boettcher, S. W.; Ivanovskaya, A.; Norvell, E.; Sherman, J. B.; Stucky, G. D.; Moskovits, M. *J. Phys. Chem. C* **2008**, *112*, 8516.

(33) Min, S. K.; Joo, O.-S.; Jung, K.-D.; Mane, R. S.; Han, S.-H. *Electrochem. Commun.* **2006**, *8*, 223. Min, S. K.; Joo, O.-S.; Mane, R. S.; Jung, K.-D.; Lokhande, C. D.; Han, S.-H. *J. Photochem. Photobiol. A* **2007**, *187*, 133.